FEBS Letters 497 (2001) 90–94 FEBS 24869

Cleavage of mitochondria-like transfer RNAs expressed in *Escherichia coli*

Véronique Bourdeau[a,1], Bruno Paquin[a,2], Robert Cedergren[a,3], Nicholas Delihas[b,*]

[a] *Département de Biochimie, Université de Montréal, C.P. 6128, Succursale Centre-Ville, Montréal, QC, Canada H3C 3J7*
[b] *Department of Molecular Genetics and Microbiology, School of Medicine, SUNY, Stony Brook, NY 11794-5222, USA*

Received 6 April 2001; accepted 13 April 2001

First published online 7 May 2001

Edited by Lev Kisselev

Abstract Mitochondrial (mt) transfer RNAs (tRNAs) often harbor unusual structural features causing their secondary structure to differ from the conventional cloverleaf. tRNAs designed with such irregularities, termed mt-like tRNAs, are active in *Escherichia coli* as suppressors of reporter genes, although they display low steady-state levels. Characterization of fragments produced during mt-like tRNA processing in vitro and in vivo suggests that these RNAs are not fully processed at their 5′ ends and are cleaved internally. These abnormal processing events may account for the low levels of mature mt-like RNAs in vivo and are most likely related to defective processing by RNase P.

Key words: Atypical tRNA; Mitochondrial tRNA; tRNA processing; RNase P; *Escherichia coli*

1. Introduction

The secondary structure of transfer RNAs (tRNAs) is generally represented by a cloverleaf. However, not all tRNAs can adopt this pattern. In particular, mitochondrial (mt) tRNAs often possess one or more 'odd' features including base substitution at conserved positions, mismatches, extended helices or lack of either the D arm or the T arm [1,2]. Different foldings for these tRNAs have been proposed where structural compensations help maintain the overall normal tertiary L-shape. These include cases where the combination of shorter connectors and a shorter D region would compensate for an extended anticodon stem, preserving a tertiary structure similar to that of the normal tRNAs [3–5]. Thus, tertiary compensations allow irregular tRNAs to interact with both the messenger RNA and the aminoacyl transfer site in the ribosome. In accordance with this, mt-like tRNAs with a longer anticodon stem and a shorter D region have been isolated for their ability to suppress a stop codon located within reporter genes [6]. Their activity in the cytoplasm of *Escherichia coli* proves the relevance of the structural compensation and the capacity of atypical tRNAs to be functional even where they are not naturally found. However their steady-state expression and their efficiency of suppression are lower than a control $tRNA^{Ala}_{su+}$ [6].

Examples of mutant tRNAs with impaired expression level have been reported where accumulation of precursor tRNA or instability of precursor and/or mature tRNAs have been found in *E. coli*, e.g. see [7]. We show here that there is defective processing of mt-like tRNAs and accumulation of a fragment resulting from cleavage within the mt-like tRNA sequence. The abnormal cleavage is most likely related to altered secondary and/or tertiary structures of the mt-like tRNAs which may block normal recognition sites and create new sites for RNase P.

2. Materials and methods

2.1. Strains

The *E. coli* strain XAC-1 [8] was used for cloning and in vivo experiments. The strain MRE 600 (*Rna*I) [9] was used to prepare the S100 extract.

2.2. Plasmids

The $tRNA^{Ala}_{su+}$ as well as two clones isolated from the original library: T7 and T37 [6], were subcloned by PCR into pBluescript SK^+ (Stratagene) (PCR protocol in [6]; other cloning protocols from [10]). The isolated clones named pBS-Ala, pBS-T7 and pBS-T37 contained the tRNA genes in front of the T3 RNA polymerase promoter.

2.3. E. coli S100 extracts

Preparation of S100 extracts from *E. coli* MRE 600 was performed as described by RajBhandary and Ghosh [11] with the following adaptations: cells were first diluted in PBS containing 1 mM phenylmethylsulfonylfluoride (PMSF) and 5 mM dithiothreitol (DTT), incubated with lysozyme for 30 min on ice, sonicated and centrifuged 2 h at 25 000 rpm (SW28; $\sim 100\,000 \times g$). We used a Q-Sepharose column (Pharmacia) and added 1 mM PMSF and 5 mM DTT to all solutions. The dialysis buffer contained 50% glycerol instead of 10% glycerol/15% polyethylene glycol.

2.4. Processing of in vitro transcribed tRNAs

Plasmids pBS-Ala, pBS-T7 and pBS-T37 were digested with *Hin*dIII (New England Biolabs, NEB), purified on agarose gel with Qiagen columns and used as a template for in vitro transcription (100 ng per reaction) with T3 RNA polymerase (50 units; Gibco) in the supplied buffer and with 0.4 mM of ATP, CTP and GTP, 0.2 mM of UTP and 15 μCi of [α-^{32}P]UTP. After 2 h at 37°C, reactions were extracted with phenol/chloroform and ethanol precipitated. Products were resolved on 7% polyacrylamide/8 M urea gels. Transcripts were located by autoradiography and eluted by incubating the gel pieces at

*Corresponding author. Fax: (1)-631-632 9797.
E-mail: nicholas.delihas@sunysb.edu

[1] Present address: DNA Learning Center, Cold Spring Harbor Laboratory, 1 Bungtown Road, P.O. Box 100, Cold Spring Harbor, NY 11724, USA; E-mail: bourdeau@cshl.org.
[2] Present address: Galileo Genomics, 6700 avenue du Parc, Suite 200, Montreal, QC, Canada H2V 4H9; E-mail: bpaquin@galileogenomics.com.
[3] Deceased. This paper is dedicated to the memory of Dr. Cedergren.

Abbreviations: mt, mitochondrial; tRNAs, transfer RNAs; PMSF, phenylmethylsulfonylfluoride; DTT, dithiothreitol

0014-5793/01/$20.00
PII: S0014-5793(01)02443-7

37°C overnight in 0.5 ml of 0.5 M ammonium acetate, 0.01 M magnesium acetate, 1 mM ethylenediaminetetraacetic acid and 0.1% sodium dodecyl sulfate. Labeled RNA was recovered by ethanol precipitation. Processing reactions were performed with ~5 μg total protein of *E. coli* S100 extract according to the conditions described by Ramesh et al. [12].

We also labeled transcripts at the 5′ end after non-radioactive in vitro transcription, dephosphorylation (calf intestine phosphatase, NEB) in the presence of RNase inhibitor and phosphorylation (T4 polynucleotide kinase, NEB) with [γ-^{32}P]ATP (30 μCi at >5000 mCi/mmol).

2.5. Northern blots

Unlabeled in vitro transcripts of tRNA^{Ala} and mt-like tRNAs treated as described for a processing study or total RNA from cultured cells were extracted and fractionated on a 6.5% polyacrylamide/8 M urea/0.1 M sodium acetate (pH 5.2) gel [6,13,14]. The RNA was transferred by electroblotting onto a nylon membrane (Hybond-N, Amersham, Buckinghampshire, UK). Hybridization with probes complementary to the anticodon region, the 5′ or 3′ end of the primary transcripts, and control 5S RNA (positions 34–53 in the *E. coli* 5S sequence) was carried out as described in McClain et al. [14] (probe sequences available upon request).

2.6. Secondary structure modeling

Standard parameters were use to fold tRNAs using the Zuker/Turner mfold program version 3.1 [15,16]. This program is available at Internet address: http://bioinfo.math.rpi.edu/~mfold/rna/.

3. Results

To investigate the low expression of mt-like tRNAs in *E. coli*, the kinetics of the processing and the stability of in vitro transcripts were investigated. Two mt-like tRNAs isolated previously were used: tRNA-T7 which has eight base pairs in the anticodon stem and tRNA-T37 which has 10 (Fig. 1) [6]. tRNA$^{Ala}_{su+}$, with the normal six base pairs in the anticodon stem, was used as a control (Fig. 1). Purified transcripts uniformly labeled with [α-^{32}P]UTP were incubated in the presence of *E. coli* S100 extract at 37°C for different times. S100 extract contains the necessary enzymatic activities to obtain mature tRNAs from normal precursor tRNA transcripts [11,12,17]. Products were separated by polyacrylamide gel electrophoresis. After 5 min incubation, new bands appear that migrate close to tRNA precursors of control tRNA$^{Ala}_{su+}$ and two mt-like tRNAs-T7 and -T37 (Fig. 2). These represent progressive exonucleolytic 3′ end processing. Two bands that migrate in the position of mature form of the three tRNAs were visible between 15 and 30 min (Fig. 2). These may represent the last steps of the 3′ processing or removal of AMP from the 3′-CCA terminus. In contrast to the processing profile of tRNA$^{Ala}_{su+}$, a high molecular weight intermediate transcript (marked by a star in Fig. 2) accumulated during the processing of mt-like tRNAs-T7 and -T37. This new band, termed 'X' fragment, had a greater intensity than the mature mt-like tRNA products. The identity of all bands was confirmed by probing Northern blots of unlabeled processing profiles with oligonucleotides corresponding to either the 5′ or the 3′ region of the full transcript (data not shown).

Southern blot analysis of plasmid DNA was performed using the 'X' fragment as a probe to determine which parts of the primary transcript were present. The plasmid containing the mt-like tRNA-T7 gene was digested with restriction enzymes in order to generate fragments containing either the whole mt-like tRNA coding region, its 5′ half, or its 3′ half. The 'X' fragment hybridized to the 5′ half of the primary transcript suggesting that the fragment contained unprocessed

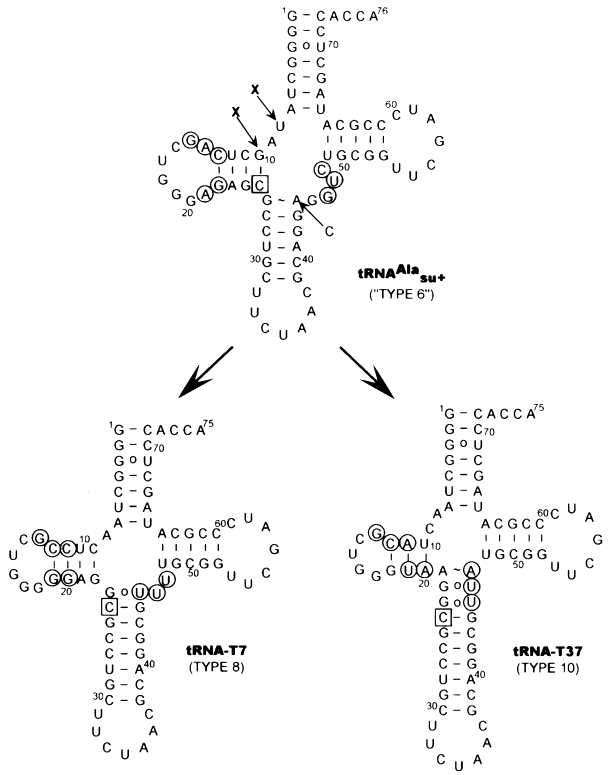

Fig. 1. Secondary structure of tRNA$^{Ala}_{su+}$ ('type 6') and mt-like tRNAs-T7 (type 8) and -T37 (type 10). The three tRNAs used in this study are represented in their cloverleaf secondary structures. The modifications made in the tRNA$^{Ala}_{su+}$ sequence to construct the library of mt-like tRNAs, from which the tRNAs-T7 and -T37 were isolated [6], are indicated. Note that both mt-like tRNAs contained an insertion of a G in position 23. Randomized positions are circled. The open square corresponds to a position allowing either A or C. 'X→': deletion in the library. 'C→': replacement of a nucleotide by a C.

5′ sequences but had lost a part of the 3′ region (data not shown). In confirmation, the 'X' fragment was visualized by probing a Northern blot of an unlabeled processing profile with an oligonucleotide complementary to the 5′ extremity of the full-length transcript.

In addition, we investigated whether the first nucleotide of the in vitro transcription was present in the 'X' fragment by comparing the processing bands obtained with transcripts labeled either internally by transcription with [α-^{32}P]UTP or end labeled at the 5′ terminus. For 5′ end labeling, unlabeled transcripts were dephosphorylated and rephosphorylated at the 5′ end with [γ-^{32}P]ATP (see Section 2). As shown in Fig. 3, high molecular weight bands corresponding to the 3′ processing of the tRNA$^{Ala}_{su+}$ were obtained when the transcripts were labeled internally or at the 5′ end but only pre-tRNA transcripts labeled internally displayed the mature tRNA. In the case of the mt-like tRNA-T7 the 3′ processed pre-tRNA as well as the 'X' fragment were visible with transcripts from both types of labeling. This indicated that the 5′ nucleotide of the precursor tRNA transcript was still a part of the 'X' fragment and that change(s) that diminished the size of the precursor tRNA occurred on the 3′ side. The above data are consistent with aberrant processing of mt-like tRNAs in vitro by RNase P.

The fate of mt-like tRNA transcripts was also investigated in vivo. Northern blot analysis using a probe that specifically recognizes the anticodon stem-loop of suppressor tRNAs showed that mt-like tRNAs were present at a significantly lower level than $tRNA^{Ala}_{su+}$ (Fig. 4, left; see also [6]). In contrast, when we used an oligonucleotide probe complementary to the first 19 nucleotides of the predicted in vivo primary transcript (nine nucleotides upstream of the mature mt-like tRNAs and 10 nucleotides within the mt-like tRNA sequence) another band was observed (Fig. 4, right). In this case, the observed band is smaller than the mature mt-like tRNA in contrast to the high molecular weight 'X' fragment transcripts found in vitro. This however is consistent with the fact that in vivo the 5′ leader region is only nine nucleotides long whereas the in vitro expression system has a 65 nucleotides leader sequence at the 5′ end due to cloning within the expression vector [6]. Thus, the fragment containing a short 5′ leader sequence of the precursor but lacking a large part of the 3′ half of the tRNA is smaller than mature mt-like tRNA. Judging by the position of the termini of the two probes, the predicted cleavage in vivo would be approximately between positions 10 and 22 in mt-like tRNAs, although a cleavage up to positions in the anticodon loop (e.g. position 35) can not be ruled out. Stringent conditions were used for Northern blot washes [14], therefore a signal would probably not be obtained using the anticodon probe if there were cleavages within the anticodon loop. The 5′ end probe contained two mismatches to the $tRNA^{Ala}_{su+}$, which explains why hybridization to mature forms of this tRNA was not as strong as the one with the mt-like tRNAs (Fig. 4).

Thus the low molecular weight band found in vivo could be equivalent to the 'X' fragment found in vitro. The appearance of these fragments suggests an explanation for the low steady-state levels of mature mt-like tRNA observed: not all precursor mt-like tRNAs are processed at the 5′ end and accumulation of mature tRNA was prevented by a cleavage of the precursor within the mt-like tRNA sequence.

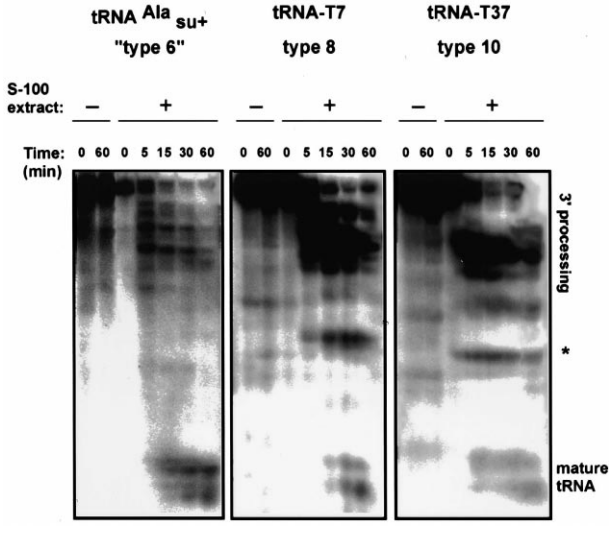

Fig. 2. In vitro processing of $tRNA^{Ala}_{su+}$ and the mt-like tRNAs-T7 and -T37. Autoradiography of 7% polyacrylamide/8 M urea gel containing samples of tRNA primary transcripts incubated for various times in the absence or in the presence of *E. coli* S100 extract. The first bands resulting from the 3′ processing and the mature tRNA bands are indicated. '*' highlights the novel cleavage product (the 'X' fragment).

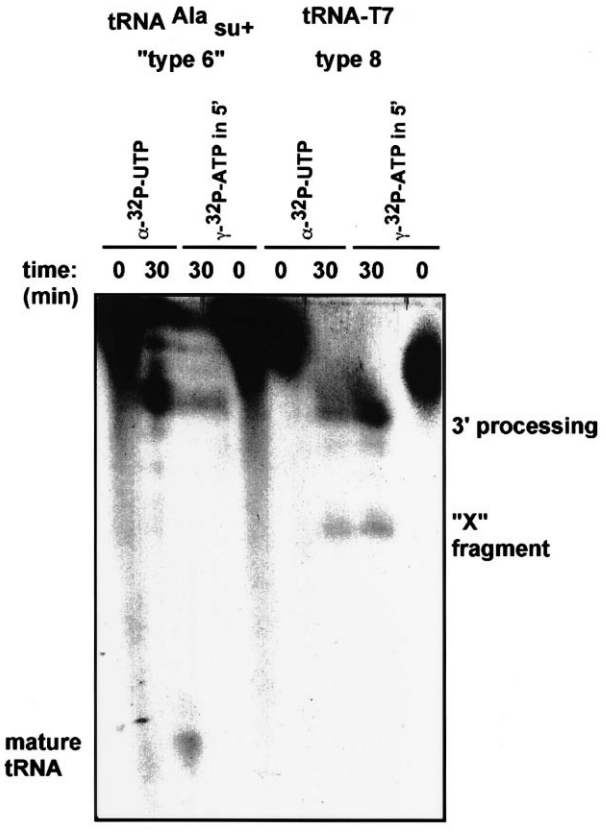

Fig. 3. In vitro processing of internally or 5′ end labeled precursor tRNA transcripts. Transcripts of $tRNA^{Ala}_{su+}$ and of mt-like tRNA-T7 were synthesized in the presence of [α-^{32}P]UTP (lanes 1, 2 for $tRNA^{Ala}_{su+}$ and lanes 5, 6 for mt-like tRNA-T7) or labeled with [γ-^{32}P]ATP after transcription (lanes 3, 4 for $tRNA^{Ala}_{su+}$ and lanes 7, 8 for mt-like tRNA-T7). Primary transcripts were incubated with *E. coli* S100 extract for 30 min and resolved on a 7% polyacrylamide/8 M urea gel. This autoradiography shows bands resulting from the 3′ processing, the complete processing (mature $tRNA^{Ala}_{su+}$) and a previously unreported cleavage (the 'X' fragment), as indicated.

4. Discussion

The low efficiency of fully processed mt-like tRNAs and accumulation of transcript fragments shown here would coincide with a decrease in recognition of the processing site by RNase P due to variant tRNA higher order structures. Defects in processing of mutant tRNAs have been observed before. Mutations in the *E. coli* gene for $tRNA^{Gly}_{2}$ display lower steady-state levels and a slower moving band on Northern blots compared to wild-type tRNA [7]. Poor recognition of the substrate by RNase P was suggested as a possible cause of low steady-state levels of mutant tRNAs and the appearance of the slow moving band, although the possible slating of fragments for degradation with polyadenylation to account for the presence of the slow moving band was not ruled out.

The internal cleavage found with two mt-like tRNAs in vivo may also be related to activity by RNase P. *E. coli* RNase P has been shown to produce polynucleotide cleavages outside of normal processing sites when mutant tRNAs or heterologous tRNAs are used as substrates [18–20]. Drosophila $tRNA^{Met}$ and two mutant Drosophila tRNAs, all of which

show internal cleavage by RNase P, appear to display alternate conformations with a long single-stranded stretch between two loops, e.g. 11 nt for $tRNA^{Met}$ [20]. The presence of different tRNA conformations may provide alternate locations for cleavage by RNase P and result in internal cleavage [20]. In this context, mt-like tRNA-T37 displays two conformations whose ΔG values are very close. Secondary structure models for mt-like tRNA-T37 produced by the Zuker program [15,16] show both the cloverleaf structure ($\Delta G = -31.9$ kcal/mol) and an alternate structure with a large 13 nt single-stranded loop ($\Delta G = -32.7$ kcal/mol) (Fig. 5). The alternate structure displays a slightly more stable free energy to the cloverleaf. Secondary structure modeling of mt-like tRNA-T7 reveals one major conformation (the cloverleaf, $\Delta G = -35.4$ kcal/mol) and several sub-optimal structures. The thermodynamically less stable structures include one that has a 9 nt single-stranded loop ($\Delta G = -32.1$ kcal/mol) (data not shown). The 'X' fragment from mt-like tRNA-T7 is less intense than that from mt-like tRNA-T37 in Northern blots (Fig. 4). Perhaps the mt-like tRNA-T7 may not be readily cleaved internally because of a low abundance of alternate structure. Analyses of the folding of control $tRNA^{Ala}_{su+}$ reveals an alternate structure with a 10 nt single-stranded loop which is less stable than the cloverleaf structure (approximately 3 kcal/mol) and represents the fifth alternate structure to the cloverleaf.

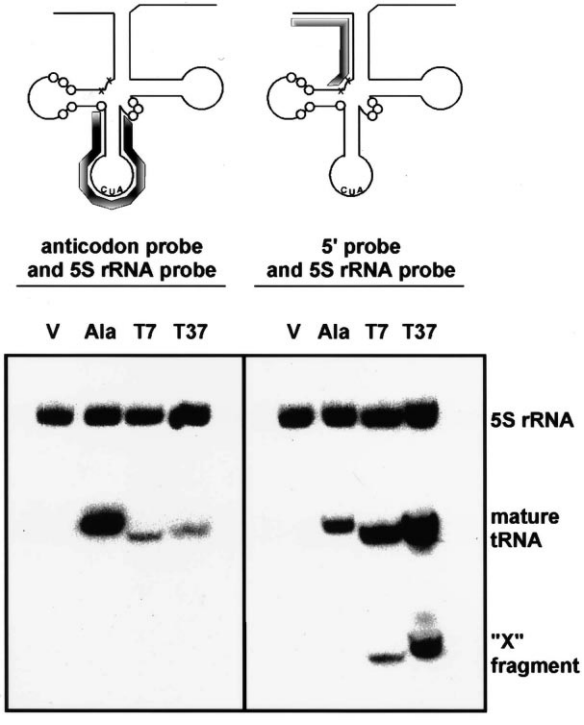

Fig. 4. In vivo identification of a fragment equivalent to the 'X' fragment. Left panel: Northern blot of 2 μg total RNA hybridized with a probe corresponding to the anticodon of the suppressor tRNAs (recognizing $tRNA^{Ala}_{su+}$, mt-like tRNA-T7 and mt-like tRNA-T37; schematized on top) as well as a probe for the 5S ribosomal RNA (rRNA; control). Right panel: Northern blot of 2 μg total RNA hybridized with a probe corresponding to the first 19 nucleotides of the in vivo mt-like tRNA primary transcripts (recognizing perfectly the mt-like tRNAs but partially $tRNA^{Ala}_{su+}$; schematized on top) as well as a probe for the 5S rRNA (control).

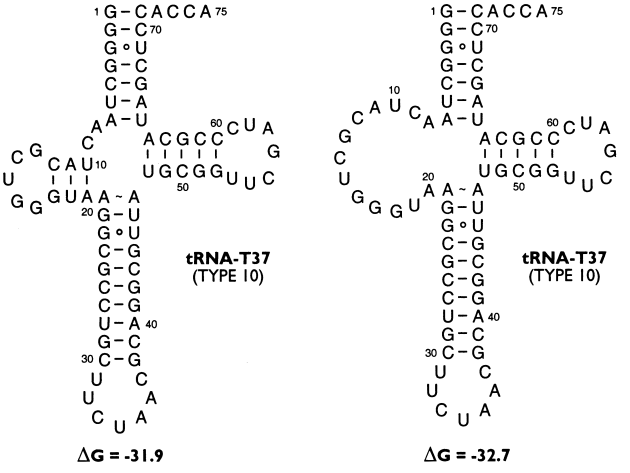

Fig. 5. Two secondary structure models for mt-like tRNA-T37. The structures were derived using the Zuker/Turner mfold version 3.1 folding program [15,16]. Left: cloverleaf model, $\Delta G = -31.9$ kcal/mol. Right: alternate model with unstructured D arm, $\Delta G = -32.7$ kcal/mol.

It is of interest that the 5′ fragments from the two mt-like tRNAs found in vivo appear stable and are not further degraded by cell nucleases. One explanation is that their resultant higher order structures may preclude exonuclease action. These fragments are rich in guanosine residues, which may produce specific intramolecular folding or intermolecular associations and thus render fragments resistant to nucleases.

Thus altered higher order structures may contribute to both low levels of processing and specific tRNA cleavage. The low efficiency of completely processed mt-like tRNAs may be related to particular tertiary structures resulting from the altered anticodon and D-loops of mt-like tRNAs. These variant tertiary structures may partially but not fully hinder recognition by RNase P. The alternate conformation model appears attractive to explain the tRNA degradation product but may also be a factor in inefficient processing, i.e. the percentage of mt-like tRNAs that have a secondary structure different from the cloverleaf may not be processed at the normal site but cleaved at an internal site.

Acknowledgements: The authors wish to express their gratitude to D. Ashburn, T. Smirlis, Dr L. Brakier-Gingras, Dr. G. Ferbeyre, Dr S.V. Steinberg and Dr. McClain for valuable help or comments. We thank Dr. Abelson, Dr. McClain and Dr. RajBhandary for strains and plasmids. This work was supported by a grant from the Natural Science and Engineering Research Council of Canada (NSERC) and a NSERC scholarship to V.B. N.D. is supported by DRAC Award, School of Medicine, SUNY, Stony Brook.

References

[1] Dirheimer, G., Keith, G., Dumas, P. and Westhof, E. (1995) in: tRNA: Structure, Biosynthesis, and Function (Söll, D. and RajBhandary, Y., Eds.), pp. 93–126, American Society for Microbiology, Washington, DC.
[2] Sprinzl, M., Horn, C., Brown, M., Ioudovitch, A. and Steinberg, S. (1998) Nucleic Acids Res. 26, 148–153.
[3] Steinberg, S. and Cedergren, R. (1994) Nat. Struct. Biol. 1, 507–510.
[4] Steinberg, S., Gautheret, D. and Cedergren, R. (1994) J. Mol. Biol. 236, 982–989.
[5] Watanabe, Y., Kawai, G., Yokogawa, T., Hayashi, N., Kumazawa, Y., Ueda, T., Nishikawa, K., Hirao, I., Miura, K. and Watanabe, K. (1994) Nucleic Acids Res. 22, 5378–5384.

[6] Bourdeau, V., Steinberg, S.V., Ferbeyre, G., Émond, R., Cermakian, N. and Cedergren, R. (1998) Proc. Natl. Acad. Sci. USA 95, 1375–1380.
[7] Herr, A.J., Atkins, J.F. and Gesteland, R.F. (1999) EMBO J. 18, 2886–2896.
[8] Normanly, J., Masson, J.M., Kleina, L.G., Abelson, J. and Miller, J.H. (1986) Proc. Natl. Acad. Sci. USA 83, 6548–6552.
[9] Cammack, K.A. and Wade, H.E. (1965) Biochem. J. 96, 671–680.
[10] Sambrook, J., Fritsch, E.F. and Maniatis, T. (1989) Molecular Cloning: A Laboratory Manual, 2nd Edn., Cold Spring Harbor Laboratory Press, Cold Spring Harbor, NY.
[11] RajBhandary, U.L. and Ghosh, H.P. (1969) J. Biol. Chem. 244, 1104–1113.
[12] Ramesh, V., Varshney, U. and RajBhandary, U.L. (1997) RNA 3, 1220–1232.
[13] Gabriel, K. and McClain, W.H. (1999) J. Mol. Biol. 290, 385–389.
[14] McClain, W.H., Jou, Y.Y., Bhattacharya, S., Gabriel, K. and Schneider, J. (1999) J. Mol. Biol. 290, 391–409.
[15] Zuker, M., Mathews, D.H. and Turner, D.H. (1999) in: RNA Biochemistry and Biotechnology (Barciszewski, J. and Clark, B.F.C., Eds.) Algorithms and Thermodynamics for RNA Secondary Structure Prediction: A Practical Guide, pp. 11–43, NATO ASI Series, Kluwer Academic Publishers, Dordrecht.
[16] Mathews, D.H., Sabina, J., Zuker, M. and Turner, D.H. (1999) J. Mol. Biol. 288, 911–940.
[17] Schedl, P., Roberts, J. and Primakoff, P. (1976) Cell 8, 581–594.
[18] Kikuchi, Y. and Sasaki, N. (1992) J. Biol. Chem. 267, 11972–11976.
[19] Park, B.H., Lee, J.H., Kim, M. and Lee, Y. (2000) Biochem. Biophys. Res. Commun. 268, 136–140.
[20] Hori, Y., Baba, H., Ueda, R., Tanaka, T. and Kikuchi, Y. (2000) Eur. J. Biochem. 267, 4781–4788.